Tetrahedron 64 (2008) 10814–10820

Contents lists available at ScienceDirect

Tetrahedron

journal homepage: www.elsevier.com/locate/tet

Novel iridium complexes as high-efficiency yellow and red phosphorescent light emitters for organic light-emitting diodes

Jun Hong Yao [a,b], Changgua Zhen [a], Kian Ping Loh [b], Zhi-Kuan Chen [a,*]

[a] Institute of Materials Research and Engineering, 3 Research Link, Singapore 117602, Singapore
[b] Department of Chemistry, National University of Singapore, 3 Science Drive 3, Singapore 117543, Singapore

ARTICLE INFO

Article history:
Received 14 February 2008
Received in revised form 24 August 2008
Accepted 11 September 2008
Available online 20 September 2008

Keywords:
Iridium complex
Phosphorescent materials
Spirobifluorene
Organic light-emitting diodes (OLEDs)

ABSTRACT

A series of novel biscyclometallated iridium complexes based on spirobifluorene ligands and acetyl acetonate (acac) ancillary ligands have been synthesized and characterized. Their electrochemical properties were investigated by cyclic voltammetry (CV). HOMO, LUMO, and energy band gaps of all the complexes were calculated by the combination of UV–vis absorption spectra and CV results. TGA and DSC results indicated their excellent thermal stability and amorphous structure. All the iridium complexes were fabricated into organic light-emitting devices with the device configuration of ITO/PEDOT:PSS (50 nm)/PVK (50 wt%):PBD (40 wt%):Ir complex (10 wt%) (45 nm)/TPBI (40 nm)/LiF (0.5 nm)/Ca (20 nm)/Ag (150 nm). Yellow to red light emission has been achieved from the iridium complexes guest materials. Complex **C1** (yellow light emission) achieved an efficiency of 36.4 cd/A (10.1%) at 198 cd/m^2 and complex **C4** (red light emission) reached external quantum efficiency of 4.6%. The slight decrease of external quantum efficiency at high current density revealed that the triplet–triplet (T_1–T_1) annihilation was effectively suppressed by the new developed complexes.

1. Introduction

Currently, organic electroluminescent materials are of interest in academic and industrial fields due to their application in light-weight, low-cost, flexible large-area optoelectronic devices.[1–4] Since the first organic light-emitting diode (OLED) was fabricated,[5] great progress has been achieved through exploration of novel high-efficient materials and optimization of device structures.[6,7] Thinner, lighter, self-emission, high efficiency, lower energy consumption, easier fabrication, and high-resolution make OLEDs very promising for full-color display.

Among the light-emitting materials for OLEDs, phosphorescent materials, which can harvest both singlet and triplet excitons have attracted great attention recently because of their higher efficiency than fluorescent materials.[8,9] Iridium complexes are the most popular choice as electrophosphorescent guest materials due to their higher efficiency and facile color tunablity comparing with other metal–ligand complexes.[10–14] However, there are some issues that need to be addressed to enhance their efficiency further. For small molecular materials, crystallization of their thin films may lead to the formation of excimers and exciplexes, which will decrease device efficiency and impair the device stability. At high doping concentrations, the intermolecular interaction in thin film will lead to self-quenching of luminescence. To address the above issues, amorphous spiro-annulated structures[15] are adopted as ligands for iridium complexes. Their 3-D bulky and steric configuration was expected to effectively suppress the close packing among the molecules in solid state.[16–18] In addition, their excellent solubility allows for solution process, which will be an advantage over other small molecules that need to be thermally deposited into films. Their good film-forming ability will offer a uniform thin film with enhanced morphological stability during device fabrication and operation. Concurrently, color tuning can be realized by modifying the conjugation length of the ligands. Here we present the synthesis and characterization of a series of spirobifluorene based ligands and the corresponding iridium complexes. The chemical structures of the complexes are shown in Figure 1. The thermal and electrochemical properties of the target iridium complexes were investigated by thermogravimetric analysis (TGA) and differential scanning calorimeter (DSC). The light emission was tuned by modification of the cyclometalated ligand structure.[11,19] The synthesized iridium complexes were employed as guest materials for OLEDs. Blended with poly(vinyl carbazole) (PVK) and 2-(4-biphenylyl)-5-(4-*tert*-butylphenyl)-1,3,4-oxadiazole (PBD) host materials, the device performance was evaluated.

* Corresponding author.
E-mail address: zk-chen@imre.a-star.edu.sg (Z.-K. Chen).

0040-4020/$ – see front matter © 2008 Elsevier Ltd. All rights reserved.
doi:10.1016/j.tet.2008.09.033

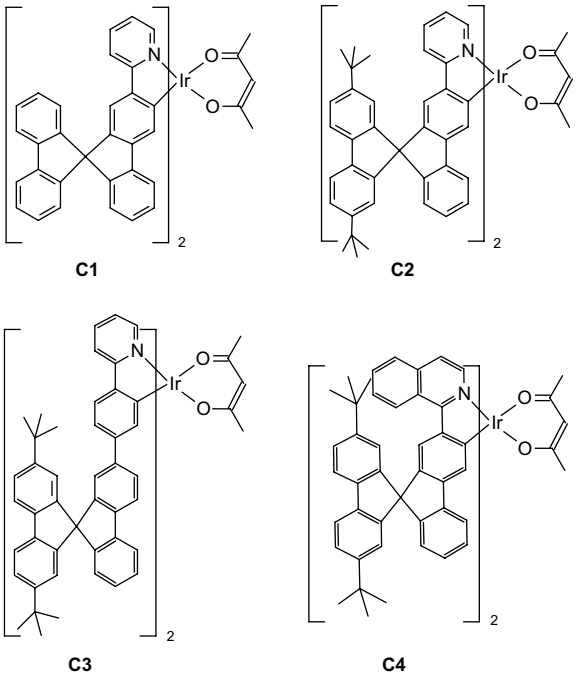

Figure 1. Structures of bis-cyclometalated Ir complexes.

2. Results and discussion

2.1. Synthesis

General synthetic routes towards the ligands are outlined in Scheme 1. First, 4,4′-di-*tert*-butylbiphenyl was synthesized from biphenyl, which reacted with *tert*-butyl chloride in dichloromethane in the presence of catalytic amount of anhydrous ferric chloride in quantitative yield.[20] 2-Bromo-4,4′-di-*tert*-butylbiphenyl **1** was obtained from 4,4′-di-*tert*-butylbiphenyl through a bromination reaction catalyzed by anhydrous ferric chloride in chloroform, proceeding in 50% yield. Compound **1** was then converted to its lithium salt 4,4′-di-*tert*-butylbiphenyl-2-lithium by reacting with *n*-butyl lithium. 2-Bromo-9-fluorenone reacted with the lithium salt of **1** in anhydrous THF solution at −78 °C, followed by a cyclization reaction, producing spirobifluorene **2** in a yield of 54%.[21] Following standard halogen–lithium reaction, 2-bis(4,4,5,5-tetramethyl-1,3,2-dioxaborolan-2-yl)-(2′,7′-di-*tert*-butyl)-9,9′-spirobifluorene **3** was synthesized in a yield of 64% from compound **2**.[22] Finally, ligands **L3** and **L4** were synthesized by following standard Suzuki coupling reactions between compound **3** with **4**[23] and 2-chloroquinoline, respectively, with yields of 74% for **L3** and 99% for **L4**.[24]

Due to the poor reactivity of 2-bromopyridine, ligands **L1** and **L2** cannot be obtained from direct coupling reaction between spirobifluorene boronic ester and 2-bromopyridine. Thus, ligands **L1** and **L2** were synthesized by different routes with ligands **L3** and **L4**. First, 2-fluorenonepyridine **5** was synthesized by oxidizing 2-fluorenepyridine in pyridine solution by saturated oxygen at room temperature, which proceeded in 97% yield. Following the cyclization procedure, compound **1** and 2-bromobiphenyl reacted with compound **8** to form spiro compounds **L1** and **L2** in yields of 69% and 48%, respectively.

A standard two-step procedure was used to synthesize the final heteroleptic Ir complexes from the ligands.[11,25–27] Firstly, the ligands were reacted with iridium chloride trihydrate in a mixture of 2-ethoxyethanol and water in the ratio of 3:1. After refluxing overnight under nitrogen, the intermediate compounds chloride-bridged dimers were obtained with medium yields. The dimers were converted to Ir complexes after reacting with acac group under reflux either in dichloromethane or in 2-ethoxyethanol in the presence of a base. The procedure is depicted in Scheme 2.

For the Ir complexes, there are two kinds of isomers, facial (*fac*) and meridional (*mer*) configuration. Meridional isomers are kinetically favored products. Their structures can be investigated by X-ray diffraction and NMR spectroscopy.[28,29] The ^{1}H NMR spectra suggest that all of the Ir complexes are formed exclusively as facial isomers, where the two ligands surrounding the iridium atom are chemically equivalent.[25] The small ancillary ligands effectively reduced the steric hindrance brought by bulky main ligands. The facial isomers are expected to have higher efficiency and better device performance comparing with the meridional isomers.[28]

2.2. Optical analysis

The UV–vis absorption spectra of the series of Ir complexes **C1**–**C4** in anhydrous dichloromethane solution are shown in Figure 2. All the complexes showed similar spectra, with three main absorption bands for each material. As can be seen, there are two low-intensity metal to ligand charge transfer (MLCT) transitions from 370 nm to 550 nm. The band at longer wavelength is assigned to triplet ^{3}MLCT d–π* excitations, while the band at shorter wavelength is attributed to singlet state ^{1}MLCT excitation. The high-intensity peaks, which start from 330 nm to 380 nm belong to the $\pi\rightarrow\pi^*$ transitions localized on the phenylpyridine-based ligands. The figures also showed that increasing the conjugation length of the cyclometalating ligand caused a red shift both of the $\pi\rightarrow\pi^*$ and $d\rightarrow\pi^*$ transition bands of the complex, which is consistent with the reported results.[11,25,26]

The photoluminescence (PL) of the complexes was measured at room temperature in anhydrous dichloromethane (DCM) solution on Luminescence Spectrometer LS50B (Perkin Elmer). The emission spectra of all the complexes are shown in Figure 3. The PL spectra can be divided into two main groups. Group 1 included complexes **C1**–**C3**, whose peak wavelengths fall into the range of 545–560 nm and they all emitted yellow light. The peak wavelength of complex **C4** was 612.5 nm and the emission light is red. The color change in light emission complies with the theory that the light emission of Ir complexes can be tuned by changing the structures of the ligands. The solution photoluminescence efficiencies (PLQE) were measured using quinoline bisulfate in 0.1 N H_2SO_4 as a standard. The PLQEs for complexes **C1**, **C2**, **C3**, and **C4** in degassed solution of toluene are 52%, 54%, 55%, and 28%, respectively. The optical properties of spirobifluorene based Ir complexes in solution are summarized in Table 1.

2.3. Thermal analysis (TGA and DSC)

The thermal stability of the Ir complexes in nitrogen was evaluated by TGA using TGA Q500 instrument (heating rate of 10 °C min^{-1}). Complex **C1** exhibited excellent thermal stability. The onset temperature of weight loss is 373 °C, and the temperature for 5% weight loss is 460 °C. The first as well as the only one weight loss is due to the cleavage of ancillary ligand (acac group). Complex **C3** showed a lower decomposition temperature than complex **C1**. The onset decomposition temperature is 260 °C. There were two stages of decomposition, which corresponded to loss of ancillary ligand (acac group) and the *tert*-butyl groups that covalently linked to the cyclometalated ligands.

Thermally induced phase transition behavior of Ir complexes was investigated by DSC under nitrogen atmosphere on a DSC Q100 instrument (scanning rate of 10 °C min^{-1}). The DSC curve revealed that the Ir complex is amorphous. On heating to 320 °C, no crystallization and melting were observed, which is matched with the

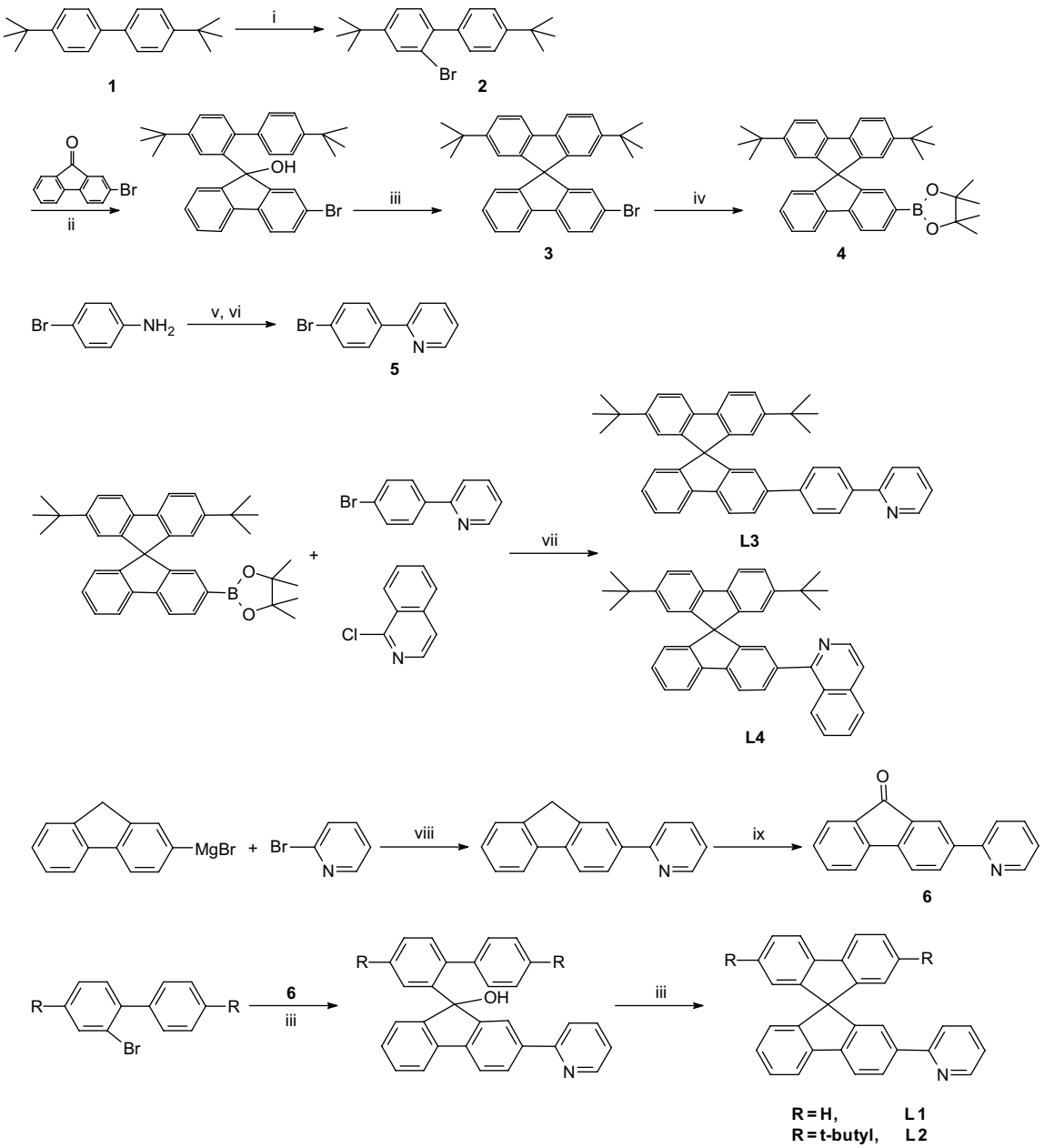

Scheme 1. Synthetic routes for the ligands. Reagents and conditions: (i) Br_2, $CHCl_3$, anhydrous $FeCl_3$, 0 °C; (ii) *n*-BuLi, THF, −78 °C; (iii) HCl, acetic acid, reflux; (iv) *n*-BuLi, THF, −78 °C, 2-isopropoxy-4,4,5,5-tetramethyl-1,3,2-dioxaborolane; (v) HCl, H_2O, $NaNO_2$, 0 °C; (vi) pyridine, 40 °C, Na_2CO_3; (vii) Na_2CO_3, toluene, $Pd(PPh_3)_4$, reflux, 24 h; (viii) THF, $Pd(PPh_3)_4$, reflux, 24 h; (ix) pyridine, O_2, overnight.

prediction that the spirobifluorene structure is amorphous. Such amorphous materials are particularly favored for OLEDs because aggregation and crystallization will affect the device stability and lifetime significantly.[30] The amorphous materials also exhibit excellent processibility, homogeneity, and isotropic properties, which are favorable for OLEDs.[31]

2.4. Electrochemical properties

The electrochemical behavior of the materials was investigated by cyclic voltammetry (CV). All the Ir complexes showed obvious oxidation peaks and underwent a reversible one-electron oxidation process, demonstrating excellent electrochemical stability of their cations. However, no reduction peak was observed. Thus, their energy band gaps were estimated from the long-wavelength absorption edge data collected from spectroscopic method. The electrochemical data and energy levels of all the Ir complexes are calculated and summarized in Table 2.

It is known that the HOMO of Ir complexes is determined by the 5d orbital of Ir with substantial mixing with the π orbitals of the ligand and LUMO is related to the π* orbitals of ligand.[25,32,33] The LUMO energy level is cyclometalating ligand dependent, which is not affected by the nature of the ancillary ligands.[34] Comparing the energy levels of **C1** and **C2**, it was found that their LUMOs are the same and **C2** showed higher HOMO, indicating that the introduction of *tert*-butyl groups decreases the energy band gap of the Ir complex due to their electron-donating abilities.[35]

2.5. Electroluminescent (EL) properties

All the OLED devices were fabricated by a combination of high vacuum thermal deposition and spin-coating on pre-cleaned ITO

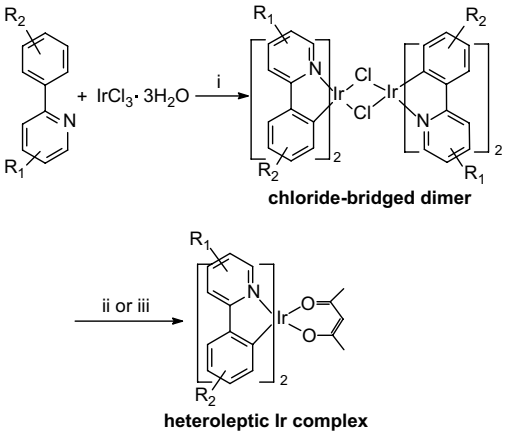

Scheme 2. Synthetic routes for the Ir(III) complexes. Reagents and conditions: (i) 2-ethoxyethanol–H_2O=3:1, reflux, 24 h; (ii) DCM, acac, tetrabutylammonium hydroxide, ethanol, reflux, 5 h; (iii) 2-ethoxyethanol, acac, Na_2CO_3, reflux, 24 h.

glass substrates employing the synthesized Ir complexes as guest materials and PVK as host material. The device configuration is ITO/PEDOT:PSS (50 nm)/PVK (50%):PBD (40%):Ir complex (10%) (45 nm)/TPBI (40 nm)/LiF (0.5 nm)/Ca (20 nm)/Ag (150 nm). The emissive Ir complexes were doped into a host polymer matrix of PVK and blended with the electron transport molecule, 2-(4-biphenylyl)-5-(4-*tert*-butylphenyl)-1,3,4-oxadiazole (PBD). The doping concentration of guest Ir complexes was fixed at 10 wt %. It is important to note that doping concentrations of guest higher than 5 wt % are typically required to efficiently quench the host luminescence and achieve good carrier transport in phosphorescent OLEDs.

All the devices display intense yellow or red emission in the range of 545–609 nm in the EL spectra, which resembled their PL spectra of the Ir complexes in DCM solution. No emission from PVK was observed, indicating that efficient energy transfer from the host materials to guest materials occurred. Furthermore, the EL emission of the device originated from the triplet excited states of the phosphors. The peak emission wavelength of EL spectra and their CIE coordinates are summarized in Table 3.

It can be seen from Figure 4 that the turn-on voltage (defined as the voltage required to give a luminance of 1 cd/m^2) of the devices is 5.8 V. The relatively higher turn-on voltage is ascribed to a low-lying HOMO level of PVK (at about −5.9 eV), and consequently,

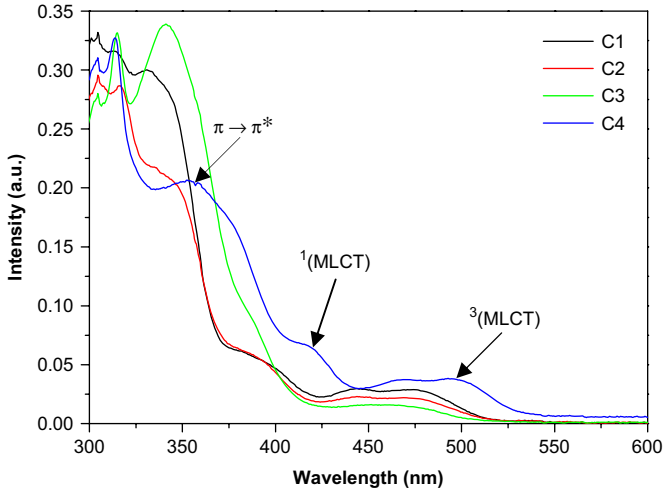

Figure 2. UV–vis absorption spectra of Ir complexes in anhydrous DCM.

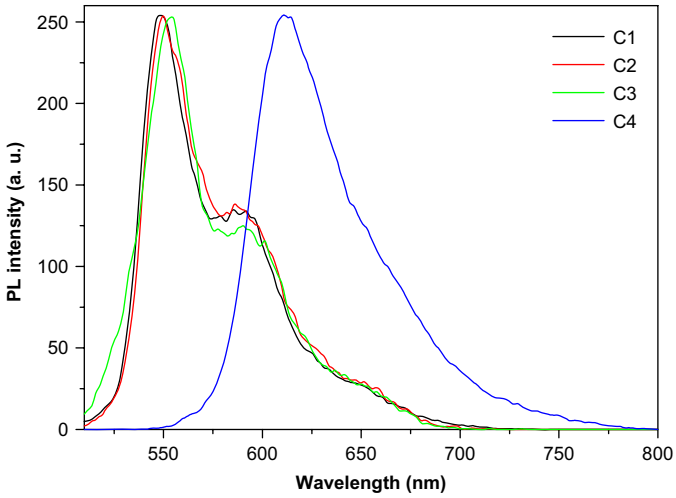

Figure 3. PL spectra of Ir complexes **C1**–**C4** in anhydrous DCM.

Table 1
Photophysical properties of Ir complexes **C1**–**C4** in anhydrous DCM

Ir Complexes	UV–vis				PL, λ_{em} (nm)
	λ_{onset} (nm)	λ_{max} (nm), $\pi\rightarrow\pi^*$	^{1}MLCT, d–π^*	^{3}MLCT, d–π^*	
C1	518.5	329.5	397.5	473.5	548.5 (591.5)
C2	535.3	340.5	390.5	468.5	550 (592)
C3	537.5	339.5	386.5	451.5	555.5 (592)
C4	610	351.5	417.5	480	612.5

Note: the data in the parentheses are the wavelength of shoulders and sub-peaks.

a large barrier for injection of holes from PEDOT:PSS, which translates into a high onset voltage.[36] Lower turn-on voltage is expected to be obtained by employing novel host materials.

The external quantum efficiency (EQE_{ext}, or η_{ext}) and luminance efficiency (LE) of complex **C1** are shown in Figure 4. Device with 10 wt % of **C1** exhibited the highest efficiency with η_{lum}=36.4 cd/A and EQE_{ext}=10.1% at 0.5 mA/cm^2 (brightness: 198 cd/m^2). When the current density increased from 0.1 mA/cm^2 to 1.0 mA/cm^2, 10.0 mA/cm^2, and 100 mA/cm^2, the external quantum efficiency of the device varied from 8.6% to 9.6%, 8.6%, and 5.8%, respectively. In a controlled experiment, when $PPy_2Ir(acac)$ was used as the dopant, the corresponding external quantum efficiencies of the device are 8.0%, 7.5%, 6.2%, and 4.2% at the four different levels of driving current. The decrease of EQE with increasing current density is attributed to increased triplet–triplet annihilation of phosphor-bound excitons and field-induced quenching effects,[37] which are

Table 2
Electrochemical properties of Ir complexes **C1**–**C4** in anhydrous DCM

Ir complexes	E_{onset} (eV)	E_{pa} (eV)	E_{pc} (eV)	HOMO (eV)	LUMO (eV)	E_g (eV)
C1	0.76	0.86	0.79	−5.16	−2.77	2.39
C2	0.69	0.83	0.73	−5.09	−2.77	2.32
C3	0.81	0.90	0.84	−5.21	−2.90	2.31
C4	0.74	0.84	0.77	−5.14	−3.11	2.03

E_{pa}: anodic peak potential, E_{pc}: cathodic peak potential.

Table 3
Summary of electroluminescence (EL)

Ir complexes	EL λ_{max} (nm)	CIE coordinates (x, y)	
C1	554.5	0.469	0.528
C2	552	0.463	0.532
C3	560	0.470	0.522
C4	609.5	0.644	0.356

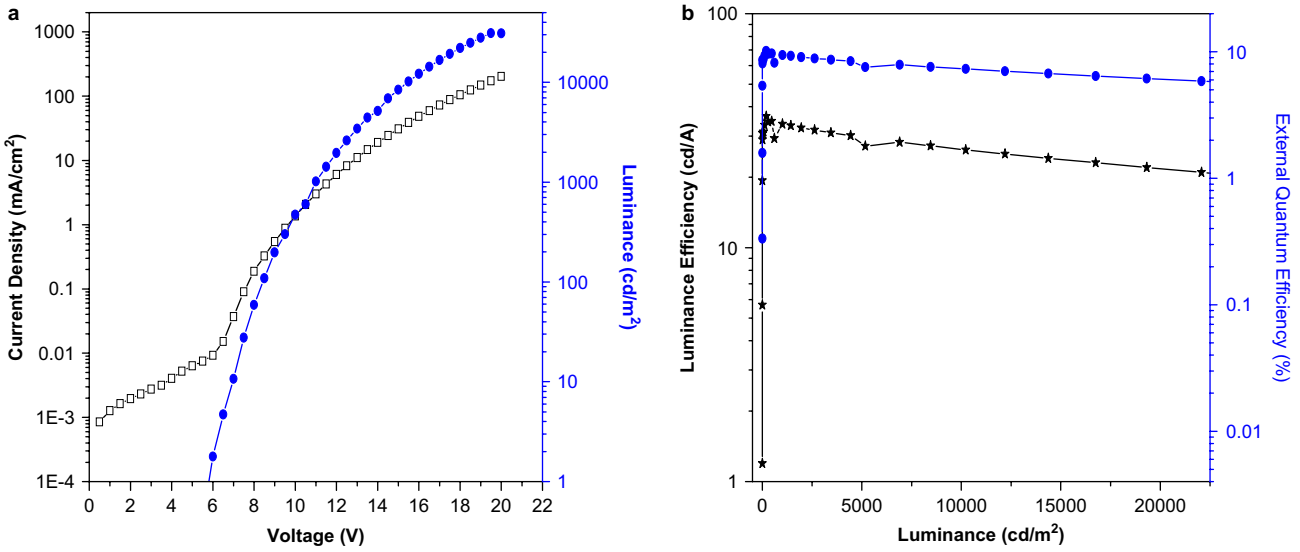

Figure 4. (a) *V–I–L* curves of device based on Ir complex **C1** and (b) luminance efficiency and external quantum efficiency of the devices based on Ir complex **C1**.

Table 4
Device characteristics of Ir complexes **C1–C4**

Ir complexes	η_{ext} (%)	$V_{Turn\text{-}on}$ (V)	λ_{max} (nm)	LE_{max} (cd/A)	L (cd/m^2) at 20 V
C1	10.1	5.8	550	36.4	30,956
C2	5.3	7.2	552	19.0	19,271
C3	5.3	6.2	560.5	19.4	15,943
C4	4.6	7.0	609	7.44	2702

key issues for phosphorescent devices. In our case, the slight drop of quantum efficiency clearly demonstrated that the T–T annihilation has been suppressed effectively by the introduction of bulky 3-D ligands through chromophore isolation[38] and preventing the energy transfer from emissive dopant to the host.[39] The device characteristics based on all the Ir complexes are summarized in Table 4.

3. Conclusion

Novel 3-D spirobifluorene ligands for Ir complexes have been designed, which suppress T–T annihilation and concentration quenching and improve the film quality in order to enhance efficiency of OLEDs and stability. Yellow to red light emissions were achieved for the Ir complexes. The thermal properties of all the Ir complexes were evaluated by TGA and DSC, indicating their good thermal stability and amorphous state. Devices were fabricated by doping the complexes at the concentration of 10 wt % into polymeric host materials PVK and PBD, showing satisfactory device performance. Complex **C1** achieved efficiency of 36.4 cd/A (10.1%) at 198 cd/m^2. The external quantum efficiency did not decrease obviously with the increasing current density, confirming that the T_1–T_1 annihilation was largely suppressed by the new designed complexes. The efficiencies of the device could be further enhanced by optimizing device structure and changing host materials.

4. Experimental

4.1. General information

All the starting materials were purchased from commercial suppliers and used directly without further purification. Tetrahydrofuran (THF) was distilled from sodium–benzophenone immediately prior to use.

^{1}H NMR and ^{13}C NMR spectra were measured in $CDCl_3$ solution on a Bruker DPX (400 MHz) NMR spectrometer with tetramethylsilane (TMS) as the internal standard. Mass spectra (MS) were recorded on a Bruker Autoflex TOF/TOF (MALDI-TOF) instrument using dithranol as a matrix. UV–vis–NIR absorption spectroscopy was measured by Shimadzu UV-3101 spectrometer at 25 °C. Fluorescence spectra were recorded on Luminescence Spectrometer LS50B (Perkin Elmer) at room temperature in anhydrous dichloromethane. The CV measurements were performed in anhydrous dichloromethane with 0.1 M tetrabutylammonium hexafluorophosphate ($TBAPF_6$) as the supporting electrolyte at a scan rate of 0.1 V/s at room temperature under the protection of nitrogen. A platinum plate was used as working electrode, a gold stick was used as counting electrode, and Al/AgCl (3 M KCl solution) was used as reference electrode.

4.2. 2-Bromo-4,4′-di-*tert*-butylbiphenyl (1)[40]

To a solution of 4,4′-di-*tert*-butylbiphenyl (3.99 g, 15 mmol) and catalyst anhydrous ferric chloride (20 mg) in chloroform (30 mL) at 0 °C was added bromine (2.4 g, 15 mmol) dissolved in chloroform (10 mL) dropwise. The reaction mixture was stirred overnight. The resultant reaction mixture was quenched with sodium carbonate until the orange color disappeared. The organic layer was separated and the water phase was washed with water and extracted with hexane (50 mL) three times. The combined organic phase was washed with saturated brine, dried over anhydrous $MgSO_4$, filtrated, and concentrated in vacuo to get a mixture of product and starting material. The conversion was estimated from proton NMR spectrum to be about 50%. The product and the starting material have the same polarity and cannot be separated by silica gel column chromatography. The starting material will not affect the next step of the reaction. Thus product mixture was not purified and was used for next reaction directly.

4.3. 2-Bromo-(2′,7′-di-*tert*-butyl)-9,9′-spirobifluorene (2)[21]

To a solution of the mixture of 4,4′-di-*tert*-butylbiphenyl and 2-bromo-4,4′-di-*tert*-butylbiphenyl (3.06 g, 5 mmol) in anhydrous THF (50 mL) was added dropwise *n*-BuLi (5 mL, 6 mmol) in hexane at −78 °C, After stirring for 1 h, the mixture was transferred to a solution of 2-bromofluorenone (1.3 g, 5 mmol) in THF (20 mL) at −78 °C and stirred overnight. Then the reaction was quenched with

water and extracted with ethyl acetate (3×50 mL). The organic layers were combined, washed with saturated brine, dried over anhydrous $MgSO_4$, filtrated, and concentrated in vacuo.

The residue was dissolved in glacial acetic acid (15 mL) and one drop of concentrated HCl was added. The mixture was heated to gentle reflux for 1 h. After the mixture was cooled down to room temperature, the precipitate was filtered and washed with water. The mixture of 2-bromo-(2′,7′-di-*tert*-butyl)-9,9′-spirobifluorene and 4,4′-di-*tert*-butylbiphenyl was separated by silica gel column chromatography eluted with hexane (R_f=0.2) to provide white solid product, 1.37 g (54%). ^{1}H NMR ($CDCl_3$, 400 MHz): δ [ppm] 7.84 (d, 1H), 7.74 (d, 3H), 7.50 (d, 1H), 7.42 (m, 3H), 7.14 (t, 1H), 6.87 (s, 1H), 6.75 (d, 1H), 6.65 (s, 2H), 1.18 (s, 18H). ^{13}C NMR ($CDCl_3$, 100 MHz): δ [ppm] 152.1, 151.3, 149.8, 148.5, 141.1, 141.0, 139.6, 131.0, 128.5, 128.0, 127.7, 125.4, 124.7, 121.5, 120.9, 120.2, 119.6, 35.2, 31.8.

4.4. 2-Bis(4,4,5,5-tetramethyl-1,3,2-dioxaborolan-2-yl)-(2′,7′-di-*tert*-butyl)-9,9′-spirobifluorene (3)[22]

To a solution of 2-bromo-(2′,7′-di-*tert*-butyl)-9,9′-spirobifluorene (1.44 g, 2.8 mmol) in anhydrous THF (14 mL) was added dropwise *n*-BuLi (4.3 mL, 5.1 mmol) at −78 °C. After stirring for 1 h, 2-isopropoxy-4,4,5,5-tetramethyl-1,3,2-dioxaborolane (1 mL, 4.8 mmol) was added. The mixture was stirred overnight. Then the reaction was quenched with water and extracted with dichloromethane (3×30 mL). The organic layer was washed with saturated brine, dried over $MgSO_4$, filtrated, and concentrated in vacuo. The residue was purified by column chromatography (silica gel, ethyl acetate–hexane=1:10) to give white solid product, 0.99 g (64%). ^{1}H NMR ($CDCl_3$, 400 MHz): δ [ppm] 7.86 (d, 3H), 7.71 (d, 2H), 7.37 (m, 3H), 7.19 (s, 1H), 7.08 (t, 1H), 6.67 (d, 1H), 6.62 (s, 2H).

4.5. 2-(4′-Bromophenyl)pyridine (4)[23]

To a solution of 4-bromoaniline (2 g, 12 mmol) in concentrated HCl (4 mL) was added slowly a solution of $NaNO_2$ (1.66 g, 24 mmol) in H_2O (3 mL) at 0 °C. The mixture was stirred at 0 °C for 1 h and pyridine (50 mL) was added. The mixture was further stirred at 40 °C for 4 h and then sodium carbonate (20 g) was added and the slurry was stirred overnight. After cooling to room temperature, water was added and the water phase was extracted with ethyl acetate. The organic layer was combined, washed with saturated brine, dried over anhydrous $MgSO_4$, filtrated, and concentrated in vacuo. Pyridine was distilled off and the residue was purified by column chromatography (silica gel, ethyl acetate–hexane=1:10) to give white solid product, 1.06 g (38%). ^{1}H NMR ($CDCl_3$, 400 MHz): δ [ppm] 8.69–8.68 (d, 1H), 7.89–7.87 (d, J=8.4 Hz, 2H), 7.8–7.74 (m, 2H), 7.71–7.69 (d, 2H), 7.61–7.59 (d, J=8.4 Hz, 2H).

4.6. 2-(Fluorenon-2-yl)pyridine (5)

A solution of 2-fluorenylmagnesium bromide (20 mmol) in anhydrous THF (60 mL) was added dropwise to a stirred mixture of 2-bromopyridine (2.39 g, 15 mmol) and $Pd(PPh_3)_4$ (0.17 g, 0.15 mmol) in anhydrous THF (60 mL) at room temperature and stirred for 1 h. Then the mixture was heated to gentle reflux under nitrogen and stirred overnight. After cooling to room temperature, the mixture was washed with water and extracted with dichloromethane (3×50 mL). The organic layer was then washed with saturated brine, dried over $MgSO_4$, and concentrated in vacuo. After purified by column chromatography (silica gel, ethyl acetate–hexane=1:20) 0.70 g (19.2%) of 2-fluorenylpyridine was obtained.

To a solution of 2-fluorenepyridine (0.4 g, 1.6 mmol) in pyridine (10 mL), tetramethylammonium hydroxide (1 mL) was added at room temperature. Then air was filled into the system and the reaction mixture was kept stirring overnight at room temperature. Then H_2SO_4 was added into the resulting suspension to eliminate the volatile pyridine. The precipitate was filtered and purified by column chromatography (silica gel, ethyl acetate–hexane=1:5); 0.41 g of yellow powder product (97%) was obtained. ^{1}H NMR ($CDCl_3$, 400 MHz): δ [ppm] 8.71–8.70 (d, 1H), 8.27–8.26 (m, 2H), 7.79–7.78 (m, 2H), 7.71–7.69 (d, 1H), 7.65–7.63 (d, 1H), 7.59–7.57 (d, 1H), 7.54–7.50 (t, 1H), 7.35–7.26 (m, 2H). ^{13}C NMR ($CDCl_3$, 100 MHz): δ [ppm] 156.5, 150.2, 145.2, 144.5, 140.9, 137.3, 135.2, 133.8, 129.7, 124.8, 123.0, 121.1, 121.0, 120.7. MS (MALDI): 258.10 (m/z), calcd for $C_{18}H_{11}NO$: 258.09.

4.7. General synthetic procedure for L1 and L2 using L1 as an example

To a solution of 2-bromobiphenyl (0.58 g, 2.5 mmol) in anhydrous THF (6 mL) was added dropwise *n*-BuLi (2.8 mL, 2.3 mmol) in hexane at −78 °C. After stirring for 1 h, the mixture was transferred to a stirred solution of 2-(fluorenon-2-yl)pyridine (0.5 g, 2 mmol) in anhydrous THF (6 mL) at −78 °C. The reaction mixture was kept stirring overnight and warmed to room temperature. Water was added to terminate the reaction. The organic layer was separated and water phase was extracted with ethyl acetate (3×20 mL). The organic layer was combined, washed with saturated brine, dried over anhydrous $MgSO_4$, filtrated, and concentrated in vacuo. The residue was dissolved in glacial acetic acid (6 mL) with one drop of concentrated HCl and the solution was heated to reflux for 1 h. After the reaction mixture was cooled to room temperature, the precipitate was filtered and washed with water. To the solution was added sodium hydroxide solution to tune to pH=7. Then, the mixed solution was extracted with ethyl acetate (3×20 mL). The organic layer was combined, washed with saturated brine, dried over anhydrous $MgSO_4$, and concentrated in vacuo. The crude product was purified by column chromatography (silica gel, hexane first, then EA–hexane=1:10) to provide light yellow solid product **L1**, 0.54 g (69%). ^{1}H NMR ($CDCl_3$, 400 MHz): δ [ppm] 8.57–8.56 (d, 1H), 8.08–8.06 (d, J=8 Hz, 1H), 7.96–7.94 (d, J=8 Hz, 1H), 7.89–7.85 (t, 3H), 7.63–7.53 (m, 2H), 7.40–7.35 (m, 4H), 7.13–7.09 (m, 4H), 6.78–6.71 (m, 3H). ^{13}C NMR ($CDCl_3$, 100 MHz): δ [ppm] 150.0, 149.1, 142.4, 141.7, 139.7, 137.0, 128.6, 128.4, 128.2, 127.4, 124.8, 124.5, 123.1, 122.3, 121.1, 120.7, 120.5. MS (MALDI): 393.138 (m/z), calcd for $C_{30}H_{19}N$: 393.151.

Compound **L2** was synthesized by the same method as **L1** with a yield of 48% as yellow powder. ^{1}H NMR ($CDCl_3$, 400 MHz): δ [ppm] 8.58 (d, 1H), 8.12–8.10 (d, 1H), 7.97–7.88 (dd, 2H), 7.73–7.71 (d, 2H), 7.63–7.52 (m, 2H), 7.39–7.36 (m, 3H), 7.31–7.26 (m, 1H), 7.14–7.09 (m, 1H), 6.72–6.68 (m, 2H), 1.14 (s, 18H). ^{13}C NMR ($CDCl_3$, 100 MHz): δ [ppm] 151.2, 150.8, 150.4, 149.7, 149.1, 143.3, 141.5, 139.7, 139.2, 137.0, 128.4, 127.8, 127.2, 125.3, 124.6, 123.0, 122.2, 121.1, 120.6, 120.5, 119.5, 35.2, 31.8. MS (MALDI): 505.260 (m/z), calcd for $C_{38}H_{35}N$: 505.276.

4.8. General procedure for the synthesis of L3 and L4, using L3 as an example

A mixture of 2-bis(4,4,5,5-tetramethyl-1,3,2-dioxaborolan-2-yl)-(2′,7′-di-*tert*-butyl)-9,9′-spirobifluorene (**4**) (0.554 g, 1 mmol), 2-(4′-bromophenyl)pyridine (**5**) (1 mmol), $Pd(PPh_3)_4$ (0.05 g, 0.043 mmol), aqueous sodium carbonate (2 M, 0.71 mL), and toluene (2.9 mL) was deoxygenated and then heated to reflux under nitrogen with stirring overnight. After the reaction mixture was cooled down to room temperature, the mixture was washed with water and extracted with ethyl acetate (3×20 mL). The organic layers were then washed with saturated brine, dried over $MgSO_4$, and concentrated in vacuo. The crude products were purified by column chromatography (silica gel, ethyl acetate–hexane=1:10) to give white solid product with the yield of 100%. ^{1}H NMR ($CDCl_3$,

400 MHz): δ [ppm] 8.70 (s, 1H), 7.97 (t, 3H), 7.92 (d, 1H), 7.76 (m, 5H), 7.59 (d, 2H), 7.42 (d, 3H), 7.28 (d, 1H), 7.13 (t, 1H), 7.04 (s, 1H), 6.72 (d, 3H), 1.17 (s, 18H). ^{13}C NMR ($CDCl_3$, 100 MHz): δ [ppm] 157.3, 151.1, 150.6, 150.3, 149.9, 149.1, 141.9, 141.6, 141.5, 140.3, 139.5, 138.3, 136.8, 128.0, 127.6, 127.5, 127.3, 126.8, 125.0, 124.4, 122.9, 122.1, 120.9, 120.5, 120.3, 35.0, 31.6, 29.9. MS (MALDI): 581.299 (*m*/*z*), calcd for $C_{44}H_{39}N$: 581.308.

Compound **L4** was synthesized with a yield of 74% as white needle crystal. ^{1}H NMR ($CDCl_3$, 400 MHz): δ [ppm] 8.35–8.33 (d, *J*=7.8 Hz, 1H), 8.10–8.02 (m, 3H), 7.93–7.91 (d, *J*=7.8 Hz, 1H), 7.76–7.74 (d, 3H), 7.69–7.64 (m, 2H), 7.48–7.38 (m, 5H), 7.14–7.11 (t, 1H), 6.74–6.71 (m, 3H), 1.14 (s, 18H). ^{13}C NMR ($CDCl_3$, 100 MHz): δ [ppm] 157.5, 151.0, 150.7, 150.2, 148.9, 148.3, 143.4, 141.3, 139.5, 139.5, 136.5, 129.8, 129.7, 128.3, 127.7, 127.7, 127.5, 127.2, 126.2, 125.1, 124.4, 123.4, 120.9, 120.5, 120.4, 119.4, 35.0, 31.6. MS (MALDI): 555.295 (*m*/*z*), calcd for $C_{42}H_{37}N$: 555.292.

4.9. General procedure for the synthesis of the Ir(III) complexes

A mixture of a ligand (1.4 mmol), iridium chloride trihydrate (0.25 g, 0.7 mmol), water (7.5 mL), and 2-ethoxyethanol (22.5 mL) was deoxygenated and then heated to reflux under nitrogen for 24 h. After cooling to room temperature, the mixture was filtrated and washed with ethanol to give product chloride-bridged dimer. Then, a mixture of the chloride-bridged dimer (0.56 g, 0.2 mmol), acetyl acetone (50 mg, 0.5 mmol), ethanol (0.3 mL), dichloromethane (15.6 mL), and tetrabutylammonium hydroxide (129 mg) was deoxygenated and heated to reflux under nitrogen for 2 h. After cooling to room temperature, the mixture was evaporated in vacuo. After column chromatographic purification (silica gel, dichloromethane), the final Ir complex products were obtained with yields ranging from 32% to 43%.

Compound **C1** was synthesized from **L1** with a yield of 32% as yellow solid. ^{1}H NMR ($CDCl_3$, 400 MHz): δ [ppm] 8.59 (d, 2H), 7.84 (d, 4H), 7.63 (m, 4H), 7.34 (m, 6H), 7.14 (m, 8H), 7.08 (m, 4H), 6.97 (d, 2H), 6.77 (d, 4H), 6.70 (d, 2H), 5.23 (s, 1H), 1.81 (s, 6H). MS (MALDI): 1075.309 (*m*/*z*), calcd for $C_{65}H_{43}N_2IrO_2$: 1075.286.

Compound **C2** was synthesized from **L2** with a yield of 43% as a yellow solid. ^{1}H NMR ($CDCl_3$, 400 MHz): δ [ppm] 8.58 (d, 2H), 7.68 (m, 8H), 7.31 (m, 6H), 7.10 (m, 4H), 6.99 (s, 2H), 6.91 (t, 4H), 6.70 (d, 2H), 6.58 (d, 2H), 6.48 (s, 2H), 5.24 (s, 1H), 1.79 (s, 6H), 1.15 (s, 18H), 0.89 (s, 18H). MS (MALDI): 1300.437 (*m*/*z*), calcd for $C_{81}H_{75}N_2IrO_2$: 1300.546.

Compound **C3** was synthesized from **L3** with a yield of 37% as yellow solid. ^{1}H NMR ($CDCl_3$, 400 MHz): δ [ppm] 8.37 (d, 2H), 7.73 (m, 6H), 7.57 (d, 2H), 7.34 (m, 8H), 7.03 (t, 2H), 6.88 (m, 4H), 6.58 (m, 6H), 6.17 (s, 2H), 5.15 (s, 1H), 1.15–1.13 (d, 36H). MS (MALDI): 1452.729 (*m*/*z*), calcd for $C_{93}H_{83}N_2IrO_2$: 1452.609.

Compound **C4** was synthesized from **L4** with a yield of 32% as red solid. ^{1}H NMR ($CDCl_3$, 400 MHz): δ [ppm] 8.69 (d, 2H), 8.44 (m, 4H), 7.91 (m, 6H), 7.72 (m, 6H), 7.54 (d, 2H), 7.39 (m, 6H), 7.14 (m, 2H), 7.02 (d, 2H), 6.72 (m, 4H), 6.35 (d, 2H), 4.90 (s, 1H), 1.34 (s, 6H), 1.22 (d, 36H). MS (MALDI): 1398.966 (*m*/*z*), calcd for $C_{89}H_{79}N_2IrO_2$: 1398.562.

References and notes

1. Shirota, Y. *J. Mater. Chem.* **2000**, *10*, 1.
2. Borchardt, J. K. *Mater. Today* **2004**, September 42.
3. Mitschke, U.; Bauerle, P. *J. Mater. Chem.* **2000**, *10*, 1471.
4. Hung, L. S.; Chen, C. H. *Mater. Sci. Eng. R.* **2002**, *39*, 143.
5. Tang, C. W.; VanSlyke, S. A. *Appl. Phys. Lett.* **1987**, *51*, 913.
6. He, G.; Pfeiffer, M.; Leo, K.; Hofmann, M.; Birnstock, J.; Pudzich, R.; Sadbeck, J. *Appl. Phys. Lett.* **2004**, *85*, 3911.
7. Shih, P.-I.; Chien, C.-H.; Chuang, C.-Y.; Shu, C.-F.; Yang, C.-H.; Chen, J.-H.; Chi, Y. *J. Mater. Chem.* **2007**, *17*, 1692.
8. Holder, E.; Langeveld, B. M. W.; Schubert, U. S. *Adv. Mater.* **2005**, *17*, 1109.
9. Kohler, A.; Wilson, J. S.; Friend, R. H. *Adv. Mater.* **2002**, *14*, 701.
10. Baldo, M. A.; Lamansky, S.; Burrows, P. E.; Thompson, M. E.; Forrest, S. R. *Appl. Phys. Lett.* **1999**, *75*, 4.
11. Lamansky, S.; Djurovich, P.; Murphy, D.; Abdel-Razzaq, F.; Lee, H.-E.; Adachi, C.; Burrows, P. E.; Forrest, S. R.; Thompson, M. E. *J. Am. Chem. Soc.* **2001**, *123*, 4304.
12. Lamansky, S.; Kwong, R. C.; Nugent, M.; Djurovich, P. I.; Thompson, M. E. *Org. Electron.* **2001**, *2*, 53.
13. Tsuzuki, T.; Shirasawa, N.; Suzuki, T.; Tokito, S. *Adv. Mater.* **2003**, *15*, 1455.
14. Beeby, A.; Bettington, S.; Samuel, I. D. W.; Wang, Z. *J. Mater. Chem.* **2003**, *13*, 80.
15. Steuber, F.; Staudigel, J.; Stossel, M.; Simmerer, J.; Winnacker, A.; Speritzer, H.; Weissortel, F.; Salbeck, J. *Adv. Mater.* **1999**, *12*, 130.
16. Geng, Y.; Datsis, D.; Gulligan, S. W.; Ou, J. J.; Chen, S. H.; Rothberg, L. J. *Chem. Mater.* **2002**, *14*, 463.
17. Kim, J. *Pure Appl. Chem.* **2002**, *74*, 2031.
18. Wong, K.-T.; Liao, Y.-L.; Su, H.-C.; Wu, C.-C. *Org. Lett.* **2005**, *7*, 5131.
19. You, Y.; Park, S. Y. *J. Am. Chem. Soc.* **2005**, *127*, 12438.
20. Rathore, R.; Burns, C. L. *J. Org. Chem.* **2003**, *68*, 4071.
21. Yu, W.-L.; Pei, J.; Huang, W.; Heeger, A. J. *Adv. Mater.* **2000**, *12*, 828.
22. Lo, S.-C.; Namdas, E. B.; Burn, P. L.; Samuel, I. D. W. *Macromolecules* **2003**, *36*, 9721.
23. Sandee, A. J.; Williams, C. K.; Evans, N. R.; Davies, J. E.; Boothby, C. E.; Kohler, A.; Friend, R. H.; Holmes, A. B. *J. Am. Chem. Soc.* **2004**, *126*, 7041.
24. Zhang, K.; Chen, Z.; Yang, C. L.; Qin, J. G.; Cao, Y. *Organometallics* **2007**, *26*, 3699.
25. Tamayo, A. B.; Alleyne, B. D.; Djurovich, P. I.; Lamansky, S.; Tsyba, I.; Ho, N. N.; Bau, R.; Thompson, M. E. *J. Am. Chem. Soc.* **2003**, *125*, 7377.
26. Chen, X.; Liao, J.-L.; Liang, Y.; Ahmed, M. O.; Tseng, H.-E.; Chen, S.-A. *J. Am. Chem. Soc.* **2003**, *125*, 636.
27. Duan, J.-P.; Sun, P.-P.; Cheng, C.-H. *Adv. Mater.* **2003**, *15*, 224.
28. Ragni, R.; Plummer, E. A.; Brunner, K.; Hofstraat, J. W.; Babudri, F.; Farinola, G. M.; Naso, F.; Cola, L. D. *J. Mater. Chem.* **2006**, *16*, 1161.
29. Mak, C. S. K.; Hayer, A.; Pascu, S. I.; Watkins, S. E.; Holmes, A. B.; Kohler, A.; Friend, R. H. *Chem. Commun.* **2005**, 4708.
30. Sun, Y.-H.; Zhu, X.-H.; Chen, Z.; Zhang, Y.; Cao, Y. *J. Org. Chem.* **2006**, *71*, 6281.
31. Jung, S.; Kang, Y.; Kim, H. S.; Kim, Y. H.; Lee, C. L.; Kim, J. J.; Lee, S. K.; Kwon, S. K. *Eur. J. Inorg. Chem.* **2004**, *17*, 3415.
32. Hay, P. J. *J. Phys. Chem. A* **2002**, *106*, 1634.
33. Ding, J.; Gao, J.; Fu, Q.; Cheng, Y.; Ma, D.; Wang, L. *Synth. Met.* **2005**, *155*, 539.
34. Chen, L.; Yang, C.; Qin, J.; Gao, J.; You, H.; Ma, D. *J. Organomet. Chem.* **2006**, *691*, 3519.
35. Ono, K.; Joho, M.; Saito, K.; Tomura, M.; Matsushita, Y.; Naka, S.; Okada, H.; Onnagawa, H. *Eur. J. Inorg. Chem.* **2006**, 3676.
36. van, A.; DijkenBastiannsen, J. J. A. M.; Kiggen, N. M. M.; Langeveld, B. M. W.; Rothe, C.; Monkman, A.; Bach, I.; Stossel, P.; Brunner, K. *J. Am. Chem. Soc.* **2004**, *126*, 7718.
37. Gong, X.; Lim, S. H.; Ostrowski, J. C.; Moses, D.; Bazan, G. C.; Heeger, A. J. *J. Appl. Phys.* **2004**, *95*, 948.
38. King, S. M.; Al-Attar, H. A.; Evans, R. J.; Congreve, A.; Beeby, A.; Monkman, A. P. *Adv. Funct. Mater.* **2006**, *16*, 1043.
39. Velusamy, M.; Thomas, K. R. J.; Chen, C.-H.; Lin, J. T.; Wen, Y. S.; Hsieh, W.-T.; Lai, C.-H.; Chou, P.-T. *Dalton Trans.* **2007**, 3025.
40. Kim, Y.-H.; Kim, H.-S.; Kwon, S.-K. *Macromolecules* **2005**, *38*, 7950.